JCTC Journal of Chemical Theory and Computation

Article

pubs.acs.org/JCTC

Free Enthalpy Differences between α-, π-, and 3_{10}-Helices of an Atomic Level Fine-Grained Alanine Deca-Peptide Solvated in Supramolecular Coarse-Grained Water

Zhixiong Lin, Sereina Riniker, and Wilfred F. van Gunsteren*

Laboratory of Physical Chemistry, Swiss Federal Institute of Technology, ETH, 8093 Zürich, Switzerland

Supporting Information

ABSTRACT: Atomistic molecular dynamics simulations of peptides or proteins in aqueous solution are still limited to the multi-nanosecond time scale and multi-nanometer range by computational cost. Combining atomic solutes with a supramolecular solvent model in hybrid fine-grained/coarse-grained (FG/CG) simulations allows atomic detail in the region of interest while being computationally more efficient. We used enveloping distribution sampling (EDS) to calculate the free enthalpy differences between different helical conformations, i.e., α-, π-, and 3_{10}-helices, of an atomic level FG alanine deca-peptide solvated in a supramolecular CG water solvent. The free enthalpy differences obtained show that by replacing the FG solvent by the CG solvent, the π-helix is destabilized with respect to the α-helix by about 2.5 kJ mol^{-1}, and the 3_{10}-helix is stabilized with respect to the α-helix by about 9 kJ mol^{-1}. In addition, the dynamics of the peptide becomes faster. By introducing a FG water layer of 0.8 nm around the peptide, both thermodynamic and dynamic properties are recovered, while the hybrid FG/CG simulations are still four times more efficient than the atomistic simulations, even when the cutoff radius for the nonbonded interactions is increased from 1.4 to 2.0 nm. Hence, the hybrid FG/CG model, which yields an appropriate balance between reduced accuracy and enhanced computational speed, is very suitable for molecular dynamics simulation investigations of biomolecules.

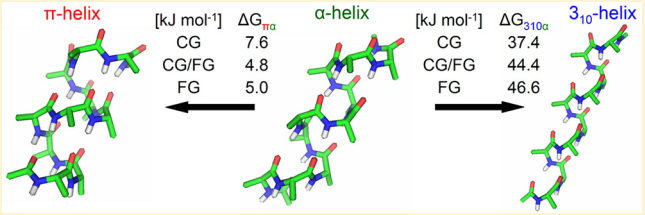

1. INTRODUCTION

During the past decades, the size of the system amenable with molecular dynamics (MD) simulations has gradually increased, allowing for the study of more complex biomolecules with this useful technique complementary to experiments. A protein in an explicitly modeled aqueous environment can currently be simulated for more than hundreds of nanoseconds. The time scale and the system size that can be studied using fully atomistic fine-grained (FG) simulations is limited, however, by the number of particle−particle interactions that must be computed. One solution is coarse graining (CG),[1−3] in which selected groups of atoms are subsumed into larger interacting beads. This will considerably reduce the number of particle−particle interactions to be calculated, smooth the energy landscape, and thus allow for an increased efficiency of up to orders of magnitude of CG versus atomistic FG simulations.

For biomolecules such as peptides or proteins, small changes in atomic detail may lead to large conformational changes, and as solutes, they present only a small part of the system to be simulated. The solvent, on the other hand, accounts for the majority of the computational cost, and the details of the solvent−solvent interactions are of less importance to the properties or processes of the biomolecules to be investigated. Thus, the combination of an atomic FG level of modeling for the solute and a supramolecular CG level for the solvent into a hybrid system may strike a proper balance between simulation accuracy and speed by reducing the computational cost of the simulation and retaining the details of the region of interest simultaneously.[3]

Developing a model spanning FG and CG levels of resolution is a nontrivial task, because a physically correct balance between the FG−FG, FG−CG, and CG−CG interactions is to be achieved.[3−10] Recently, a relatively simple procedure employing a minimal reparametrization of the FG−CG interactions while leaving FG−FG and CG−CG interactions untouched was proposed by Riniker and van Gunsteren.[10] The CG water model[11] used represents five FG water molecules by one CG bead with two interaction sites. The two oppositely charged sites connected by an unconstrained bond form a polarizable dipole, thus allowing the explicit treatment of the electrostatic interactions.[11] Only two parameters for the FG/CG interactions, i.e., the C_{12} parameter of the dipole particle of the CG bead and the dielectric permittivity for the FG−CG interactions, were calibrated based on simulations of mixtures of FG and CG water.[10] The proposed hybrid model reproduces the experimental density, surface tension, and static relative dielectric permittivity as well as the free enthalpy of solvation of a FG water molecule and FG alkanes.[10]

The hybrid FG/CG model was tested for four proteins solvated in CG water.[12,13] Analysis of the 20 ns of simulations

Received: November 30, 2012
Published: January 22, 2013

showed the preservation of the secondary structure elements, and similar backbone atom-positional root-mean-square deviations (RMSD) from the crystal structure, root-mean-square fluctuations (RMSF) of C_α atoms, and radii of gyration as in the fully atomistic simulations. The main difference observed between the use of a CG instead of an FG solvent was an increased occurrence of hydrogen bonds involving protein side-chain atoms due to the lack of hydrogen-bonding capacity of the solvent beads.[12] Introduction of an FG water layer around the solute led to a decrease of hydrogen bonding between side chains. A layer thickness of 0.8 nm was found to be sufficient to recover the properties of the fully atomistic simulation.[13]

In this article, we further test the hybrid FG/CG model by calculating the free enthalpy differences between different helical conformations, i.e., α-, π-, and 3_{10}-helices, of an atomic level FG alanine deca-peptide solvated in a supramolecular CG water solvent. The free enthalpy differences were calculated using enveloping distribution sampling (EDS).[14−21] The results are compared with the ones obtained from corresponding simulations of the peptide in an atomic level FG water solvent[19] in terms of the relative free enthalpy differences between the different helices and the dynamics of the peptide.

2. MOLECULAR MODEL AND COMPUTATIONAL METHOD

2.1. Molecular Model. The system studied is an alanine deca-peptide capped at both termini with methyl groups, acetyl-$(Ala)_{10}$-N-methyl, solvated in water. The atomistic GROMOS force field 53A6[22] was used for the peptide, and the simple-point-charge (SPC)[23] water model was used as the atomistic fine-grained (FG) solvent. The coarse-grained (CG) solvent model is described in detail in ref 11. The calibration of the parameters for the FG−CG interactions is described in ref 10.

2.2. Definition of End-State Hamiltonians and Conformational Sets. Different end-state Hamiltonians *A*, *B*, and *C*, which restrain the peptide to α-, π-, and 3_{10}- helical conformations, respectively, were defined using atom−atom distance restraining potential energy terms. These are defined as an attractive half-harmonic function applied to the hydrogen-bonding pairs of H and O atoms that characterize the respective helices.[19] The force constants and the reference distances for these terms in the different end-state Hamiltonians are listed in Tables S1−3.

The conformational sets α and β corresponding to the helices were defined through the atom-positional root-mean-square deviation (RMSD) of the backbone atoms (N, C_α, C) of the peptide (including the two terminal residues) from the ideal helices, which were defined through the φ and ψ backbone torsional-angle values −57.8° and −47.0° for the α-helix, −57.0° and −70.0° for the π-helix, and −49.0° and −27.0° for the 3_{10}-helix, followed by an energy-minimization in a vacuum. Conformations belong to set α if

$$\mathrm{RMSD}(\vec{r}^{\,N_{bb}}, \vec{r}_\alpha^{\,N_{bb}}) \leq \mathrm{RMSD}_\alpha^{thres} \text{ and } \mathrm{RMSD}(\vec{r}^{\,N_{bb}}, \vec{r}_\beta^{\,N_{bb}}) > \mathrm{RMSD}_\beta^{thres} \quad (1)$$

they belong to set β if

$$\mathrm{RMSD}(\vec{r}^{\,N_{bb}}, \vec{r}_\alpha^{\,N_{bb}}) > \mathrm{RMSD}_\alpha^{thres} \text{ and } \mathrm{RMSD}(\vec{r}^{\,N_{bb}}, \vec{r}_\beta^{\,N_{bb}}) \leq \mathrm{RMSD}_\beta^{thres} \quad (2)$$

where $\vec{r}^{\,N_{bb}} = (\vec{r}_1, \vec{r}_2, \ldots \vec{r}_{N_{bb}})$ denotes a configuration of the N_{bb} backbone atoms of the solute and the subindex α denotes the conformation α. In a two-state EDS simulation of the α-helix and π-helix, sets α and β are the α-helix and π-helix, respectively, and in a two-state EDS simulation of the α-helix and 3_{10}-helix, sets α and β are the α-helix and 3_{10}-helix, respectively. The RMSD threshold value $\mathrm{RMSD}_\xi^{thres}$ was set to 0.15 nm for all three helices.[19]

2.3. Enveloping Distribution Sampling (EDS) Simulations. The potential energy of the EDS reference-state Hamiltonian V_R of the *N* particles of the system is defined as[19]

$$\begin{aligned} V_R(\vec{r}^{\,N}; s, E_{BA}^R) &= -k_B T s^{-1} \ln\{e^{-s(V_A^{rest}(\vec{r}^{\,N}) - E_A^R)/k_B T} \\ &\quad + e^{-s(V_B^{rest}(\vec{r}^{\,N}) - E_B^R)/k_B T}\} + V^{phys}(\vec{r}^{\,N}) \\ &= V^{EDS,rest}(\vec{r}^{\,N}; s, E_{BA}^R) + V^{phys}(\vec{r}^{\,N}) \end{aligned} \quad (3)$$

where V_A^{rest} and V_B^{rest} are the restraining potential energy functions of the two end states, k_B is Boltzmann's constant, T is the temperature, s is a smoothness parameter, and $E_{BA}^R = E_B^R - E_A^R$ is an energy offset parameter difference. The (GROMOS) force field is denoted by V^{phys}.

The free enthalpy difference between the two conformational sets, i.e. $\Delta G_{\beta\alpha}$, was calculated as[19]

$$\begin{aligned} \Delta G_{\beta\alpha} &= G_\beta - G_\alpha \\ &= -k_B T \ln\left\{ \frac{\left\langle e^{+V^{EDS,rest}/k_B T} \right\rangle_{R,set\beta}}{\left\langle e^{+V^{EDS,rest}/k_B T} \right\rangle_{R,set\alpha}} \cdot \frac{N_\beta(V_R)}{N_\alpha(V_R)} \right\} \end{aligned} \quad (4)$$

where N_α denotes the number of configurations belonging to set α in the simulation of the reference state and $\langle \ldots \rangle_{R,set\alpha}$ denotes an ensemble average over these configurations. The statistical uncertainties were estimated using block averaging.[24]

2.4. Simulation Setup and Analysis. The equilibrated configuration of the peptide from the fully atomistic simulation[19] was used as a starting structure. The peptide was solvated in a cubic box with a minimum distance to the wall of 1.4 nm, resulting in 661 CG solvent beads. After a steepest descent energy minimization to remove close contacts between solute atoms and solvent beads, an equilibration scheme was carried out in three steps.[12] The initial velocities were generated from a Maxwell distribution at 300 K. In the first 100 ps, the peptide atoms were positionally restrained with a force constant of 2.5×10^4 kJ mol^{-1} nm^{-2}, and the volume was held constant. In the second step, a constant pressure simulation of 250 ps length was carried out with a position-restraining force constant of 2.5×10^2 kJ mol^{-1} nm^{-2}, and subsequently a 250 ps simulation was performed without any position restraints. In all three steps, hydrogen-bond restraining was applied.

In the simulations with an atomistic water layer, a layer thickness of 0.8 nm was chosen.[13] An equilibrated configuration from the fully atomistic simulation was used to select the molecules of the FG water layer, resulting in 284 FG water molecules around the peptide. CG water beads were then added until a similar volume to that in the simulation of the peptide in pure FG water was reached, resulting in 604 CG beads. In order to keep the FG water molecules around the peptide, attractive half-harmonic distance restraints beyond a distance of 1.8 nm were applied between the oxygen atoms of the FG water molecules and the center of mass of the peptide approximated by the center of mass of the C_α atoms of residues

4, 5, 6, and 7. The force constant for the distance restraints was in all cases[13] 300 kJ mol^{-1} nm^{-2}. After a steepest descent energy minimization to remove close contacts between FG solvent molecules and CG solvent beads, an initialization and equilibration scheme was carried out in three steps as described above.

All further simulations were performed at constant temperature and pressure using the GROMOS11 simulation package.[25−29] The simulation periods are shown in Table 1. The temperature was maintained close to its reference value T = 300 K by weak coupling[30] to a temperature bath with a relaxation time of 0.1 ps. The solute and solvent were coupled separately to the heat bath. The pressure was maintained close to its reference value P = 1.013 bar (1 atm) by weak coupling[30] to a pressure bath with a relaxation time of 0.5 ps and using the isothermal compressibility κ_T = 4.575 × 10^{-4} (kJ mol^{-1} nm^{-3})$^{-1}$. Newton's equations of motion were integrated using the leapfrog scheme with a time step of 2 fs. The bond lengths of the solute and the geometry of the atomistic water molecules were constrained to the ideal values applying the SHAKE algorithm.[31] A twin cutoff method was used for the nonbonded interactions with a short-range cutoff radius of 1.4 nm and an intermediate-range cutoff radius of 2.0 nm.[10−13] For the electrostatic interactions within the cutoff sphere, a relative dielectric permittivity ε_{CS}^{mix} = 2.3 was used for the FG−CG interactions,[10] ε_{CS}^{CG} = 2.5 for the CG−CG interactions,[11] and ε_{CS}^{FG} = 1 for the FG−FG interactions.[22] A reaction-field force[32] was applied using the experimental relative dielectric permittivity ε_{rf} = 78.5. When calculating the Coulomb interactions between atoms, pairs of atoms that are covalently bound (first) neighbors or second neighbors or in particular cases third neighbors are excluded.[22] However, when calculating the reaction-field interaction, these pairs of covalently bound neighbors should not be excluded.[32] We note that in the simulations of ref 19, these contributions to the reaction field by the covalently bound atoms were inadvertently omitted.

Table 1. Overview of the EDS Simulations

simulation name	solvent[a]	helices	time [ns]	EDS parameters s/ E_B^R [kJ mol^{-1}] obtained or used	$\Delta G_{\pi\alpha}$ or $\Delta G_{310\alpha}$ [kJ mol^{-1}][b]
update1	CG	α/π	139 × 0.15	0.09/23.8	
EDS1	CG	α/π	51	0.09/23.8	7.6 ± 0.7
update2	CG	$\alpha/3_{10}$	256 × 0.15	0.04/51.5	
EDS2	CG	$\alpha/3_{10}$	101	0.04/51.5	37.4 ± 1.5
update3	layer 0.8 nm	α/π	132 × 0.15	0.20/11.2	
EDS3	layer 0.8 nm	α/π	51	0.20/11.2	4.8 ± 0.7
update4	layer 0.8 nm	$\alpha/3_{10}$	256 × 0.15	0.03/69.5	
EDS4	layer 0.8 nm	$\alpha/3_{10}$	101	0.03/69.5	44.4 ± 1.8

[a]Solvent: the coarse-grained water solvent with an atomistic water layer of 0.8 nm (layer 0.8 nm) or the coarse-grained water solvent (CG). [b]The results obtained from the EDS simulations in the fully fine-grained (FG) solvent are[19] $\Delta G_{\pi\alpha}$ = 5.0 ± 0.8 kJ mol^{-1} (averaged results and statistical uncertainties over four different EDS free-enthalpy simulations) and $\Delta G_{310\alpha}$ = 46.6 ± 1.5 kJ mol^{-1} (calculated from a 100 ns EDS free-enthalpy simulation which was extended from the 50 ns simulation in ref. [19]).

Trajectory coordinates and energies were stored at 1 ps intervals for analysis. In the EDS free-enthalpy evaluation simulations, the first ns was treated as an equilibration period, and the last 50 or 100 ns were used to calculate the free enthalpy differences. Atom-positional root-mean-square deviations (RMSD) between peptide configurations were calculated after translational superposition of solute centers of mass and rotational least-squares fitting of the atomic coordinates of all backbone atoms of the alanine deca-peptide.

3. RESULTS AND DISCUSSION

The EDS update simulation update1 of the α-helix and π-helix in the coarse-grained (CG) supramolecular solvent (Table 1) is shown in Figure S1, and the corresponding EDS free-enthalpy evaluation simulation EDS1 is shown in Figure 1. Many transitions between the α-helix and π-helix occurred during the 50 ns simulation period. The resulting free enthalpy difference $\Delta G_{\pi\alpha}$ is 7.6 ± 0.7 kJ mol^{-1}. Another EDS free-enthalpy evaluation simulation with slightly different EDS parameters (Supporting Information Figures 2 and 3) gave $\Delta G_{\pi\alpha}$ = 7.7 ± 0.6 kJ mol^{-1}, indicating good convergence of the free enthalpy values.

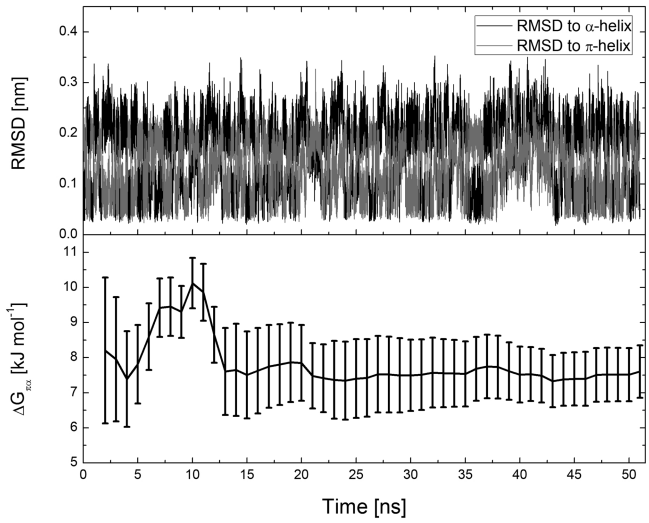

Figure 1. Time evolutions of backbone atom-positional RMSD of the peptide with respect to the α-helix or π-helix and free enthalpy difference $\Delta G_{\pi\alpha}$ between the π-helix and α-helix in the EDS evaluation simulation EDS1 of the peptide in the coarse-grained water solvent.

The transitions between the two helices in the simulation EDS1 occur on a smaller time scale than the ones in the simulations using the same solute force field for the peptide in the fully atomistic fine-grained (FG) water solvent.[19] The effect of the CG water solvent on the transitions between the helices is 2-fold: first, the CG solvent smoothes the potential energy surface and thus speeds up the diffusion of the system. Second, the CG beads cannot form hydrogen bonds with the peptide, making it more difficult to break up intrapeptide hydrogen bonds and thus decreasing the transitions. In the present case, the transitions are enhanced so the former effect is dominant.

The EDS update simulation update2 of the α-helix and 3_{10}-helix in the CG solvent (Table 1) is shown in Figure S4, and the corresponding EDS free-enthalpy evaluation simulation EDS2 is shown in Figure 2. Since the convergence of $\Delta G_{310\alpha}$ is slower than that of $\Delta G_{\pi\alpha}$, the simulation was carried out for

dx.doi.org/10.1021/ct3010497 | J. Chem. Theory Comput. 2013, 9, 1328−1333

101 ns. The resulting free enthalpy difference $\Delta G_{310\alpha}$ is 37.4 ± 1.5 kJ mol^{-1}.

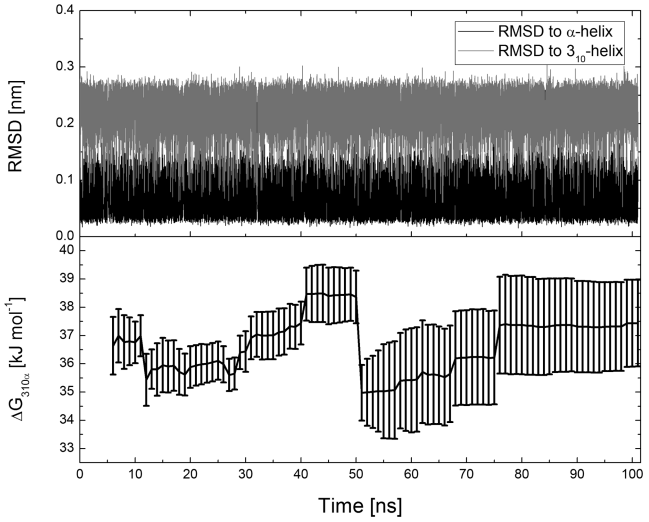

Figure 2. Time evolutions of backbone atom-positional RMSD of the peptide with respect to the α-helix or 3_{10}-helix and free enthalpy difference $\Delta G_{310\alpha}$ between the 3_{10}-helix and α-helix in the EDS evaluation simulation EDS2 of the peptide in the coarse-grained water solvent.

Comparing with the FG water solvent,[19] for which $\Delta G_{\pi\alpha}$ = 5.0 ± 0.8 kJ mol^{-1} and $\Delta G_{310\alpha}$ = 46.6 ± 1.5 kJ mol^{-1} were obtained (Table 1), the CG solvent destabilizes the π-helix with respect to the α-helix by about 2.5 kJ mol^{-1} and stabilizes the 3_{10}-helix with respect to the α-helix by about 9 kJ mol^{-1}. The 3_{10}-helix contains the largest number of intrapeptide hydrogen bonds among the three helical conformations and may be stabilized relative to the other conformations due to the lack of hydrogen-bonding capacity of the CG solvent beads.

The EDS simulations were also carried out for the peptide in the CG water solvent with an atomistic water layer of 0.8 nm. The EDS update simulation update3 of the α-helix and π-helix is shown in Figure S5, and the corresponding EDS free-enthalpy evaluation simulation EDS3 is shown in Figure 3. There are less transitions between the α-helix and π-helix than in pure CG solvent (Figure 1), the number being similar to that in fully FG solvent.[19] The free enthalpy difference $\Delta G_{\pi\alpha}$ calculated from EDS3 is 4.8 ± 0.7 kJ mol^{-1}, which is almost identical to the $\Delta G_{\pi\alpha}$ result obtained from the EDS simulation of the peptide in the fully FG solvent.[19]

Time evolutions of the free enthalpy differences $\Delta G_{\pi\alpha}$ calculated from the simulations of the peptide in the fully FG solvent, the CG solvent with the atomistic water layer of 0.8 nm, and the CG solvent are compared in Figure 4. The convergence of the result from the simulation of the peptide in the CG solvent is much faster than from the simulations using the other solvent models. This is in line with the larger number of transitions between the helices observed for the peptide in the CG solvent. The results obtained from the simulations of the peptide in the CG solvent with the FG layer and the fully FG solvent converge to very similar values (Figure 4).

The EDS simulations of the α-helix and 3_{10}-helix in the CG solvent with the 0.8 nm FG layer are shown in Figure S6 for update4 and Figure S7 for EDS4. The resulting free enthalpy difference $\Delta G_{310\alpha}$ is 44.4 ± 1.8 kJ mol^{-1} (Table 1), which is

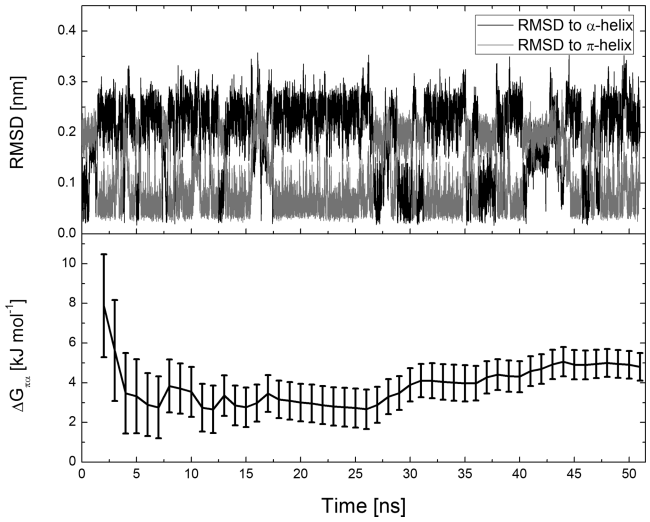

Figure 3. Time evolutions of backbone atom-positional RMSD of the peptide with respect to the α-helix or π-helix and free enthalpy difference $\Delta G_{\pi\alpha}$ between the π-helix and α-helix in the EDS evaluation simulation EDS3 of the peptide in the coarse-grained water solvent with an atomistic water layer of 0.8 nm.

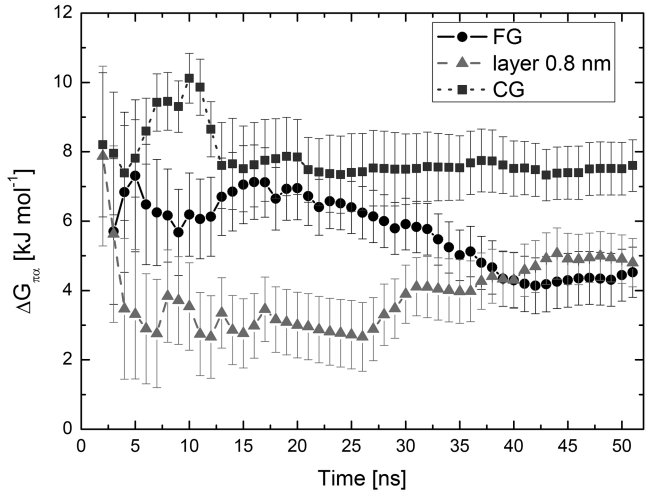

Figure 4. Time evolutions of free enthalpy difference $\Delta G_{\pi\alpha}$ between the π-helix and α-helix in the EDS free-enthalpy evaluation simulations of the peptide in the fully atomistic fine-grained solvent (FG), in the coarse-grained solvent with an atomistic water layer of 0.8 nm (layer 0.8 nm), and in the fully coarse-grained supramolecular solvent (CG).

within the statistical uncertainty of the result obtained in the FG solvent (Table 1).[19]

As in the previous study,[12,13] more negative intrapeptide electrostatic energies and less negative intrapeptide Lennard-Jones energies in the simulations of the CG solvent were observed (Table S4), due to the stronger intrapeptide hydrogen bonding. Adding a 0.8 nm FG layer, the intrapeptide potential energies and their components are comparable to those of the peptide in the fully FG solvent (Table S4).

These results show that not only the structural properties[13] but also the dynamic and thermodynamic properties can be recovered by adding a FG layer of 0.8 nm when using the CG solvent. This comes at the cost of losing a factor of 2−3 in computational efficiency (Table 2). Yet, the gain is still significant; i.e., the simulations of the peptide in the CG solvent are 9 times faster than in the FG solvent, and adding a 0.8 nm

dx.doi.org/10.1021/ct3010497 | J. Chem. Theory Comput. 2013, 9, 1328−1333

Table 2. Number of Fine-Grained (FG) Water Molecules and Coarse-Grained (CG) Water Beads in the EDS Simulations and the Corresponding Speedup Factors

solvent[a]	FG/CG	initial box size [nm]	cutoffs	speed up factor
FG	3204/0	4.60	0.8/1.4 nm	1
layer 0.8 nm	284/604	4.68	1.4/2.0 nm	4
CG	0/661	4.69	1.4/2.0 nm	9

[a]Solvent: the fully atomistic fine-grained solvent (FG), the coarse-grained solvent with an atomistic water layer of 0.8 nm (layer 0.8 nm), and the fully coarse-grained supramolecular solvent (CG).

FG layer, the simulations are still 4 times faster (Table 2). We note that these speedup factors were estimated using the simulations with much larger cutoff distances for nonbonded interactions (Table 2) in the CG solvent.

In all three solvent models, the relative stabilities of the three helices are the α-helix > the π-helix $\gg$ the 3_{10}-helix. This may be explained by the relative sizes of the dipole moments of the helices shown in Figure 5. The α-helix has the largest dipole,

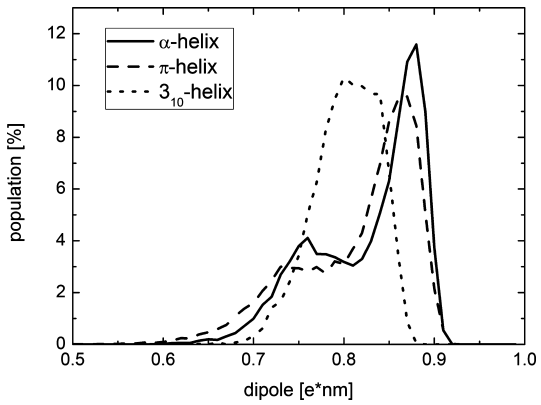

Figure 5. Distributions of the dipole moments of three helical conformations in the EDS free-enthalpy evaluation simulations. Distributions of the α- and π-helices are averaged over the configurations belonging to the α- or π- helix, respectively, sampled in the EDS simulation EDS1, the distribution of the 3_{10}-helix is averaged over the configurations belonging to 3_{10}-helix in the EDS simulation EDS2. The averaged dipole moments are 0.83, 0.82, and 0.80 e·nm for the α-helix (solid line), π-helix (dashed line), and 3_{10}-helix (dotted line), respectively.

and the 3_{10}-helix the smallest one. Since the side chains of the alanine deca-peptide are hydrophobic, the helical conformation with the smallest solvent accessible surface area (SASA) is expected to be the most stable. Figure 6 shows that the π-helix has the lowest SASA value and the 3_{10}-helix the largest one. Together with the size of the dipole moments, this explains the comparable free enthalpies of the α- and π-helices and the much larger value for the 3_{10}-helix.

In a different context, the free enthalpy differences between the three helices were calculated using the ball-and-stick local elevation umbrella sampling method.[33] The results were 4, 0, and 12 kJ mol^{-1} for the relative free enthalpies of the π-, α-, and 3_{10}- helix of the alanine deca-peptide using the GROMOS 53A6 force field solvated in atomistic SPC water solvent. The much lower $\Delta G_{310\alpha}$ is probably due to a different definition of helical conformations used in that study[33] based on a sum of backbone φ-/ψ-dihedral-angle values instead of the backbone atom-positional RMSD.

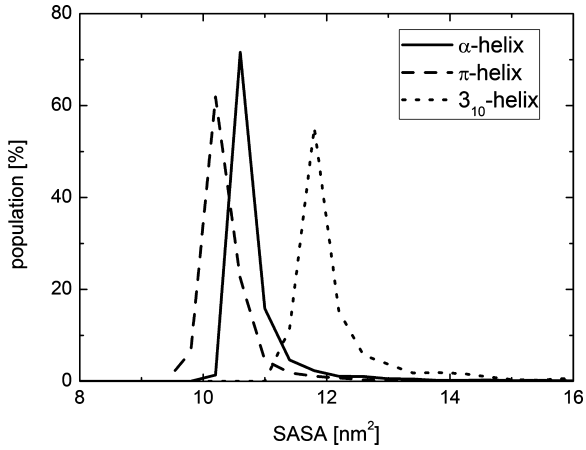

Figure 6. Distributions of the solvent-accessible surface area (SASA) of the three helical conformations in the EDS free-enthalpy evaluation simulations. Distributions of the α- and π- helices are averaged over the configurations belonging to the α- or π-helix, respectively, sampled in the EDS simulation EDS1; the distribution of the 3_{10}-helix is averaged over the configurations belonging to the 3_{10}-helix in the EDS simulation EDS2. The averaged SASA values are 10.8, 10.4, and 12.2 nm^2 for the α-helix (solid line), π-helix (dashed line), and 3_{10}-helix (dotted line), respectively.

4. CONCLUSION

The free enthalpy differences between different helical conformations, i.e., α-, π-, and 3_{10}-helices, of a fine-grained (FG) atomic-level resolution alanine deca-peptide solvated in a coarse-grained (CG) supramolecular level resolution water solvent were calculated using enveloping distribution sampling (EDS).

Solvated in CG water, more transitions between the helices in the two-state EDS simulations of the alanine deca-peptide are observed than when solvated in fine-grained (FG) water solvent, due to a smoother potential energy surface in the presence of the CG solvent. In terms of relative stabilities between different helices, the π-helix is destabilized with respect to the α-helix by about 2.5 kJ mol^{-1}, and the 3_{10}-helix is stabilized with respect to the α-helix by about 9 kJ mol^{-1}, when using the CG solvent instead of the FG solvent, because of the stronger intrapeptide hydrogen bonding in the simulations of the CG solvent due to a lack of hydrogen-bonding capacity of the CG beads.

The introduction of a FG water layer around the deca-peptide solvated in CG water resulted in free enthalpy differences and numbers of transitions that are similar to the values obtained for the peptide in fully FG water. This implies that not only the solute atoms determine these quantities but also a shell of solvent molecules around them. With a sufficiently thick FG solvent layer, however, both the dynamic and thermodynamic properties of a solute can be recovered, while the mixed FG/CG solvent still renders the simulations computationally more efficient.

■ ASSOCIATED CONTENT

Ⓢ Supporting Information

Hydrogen-bond populations of the end-state simulations, nonbonded interaction energies in the EDS simulations, and some EDS parameter update and free-enthalpy evaluation simulations are available. This information is available free of charge via the Internet at http://pubs.acs.org.

AUTHOR INFORMATION

Corresponding Author

*E-mail: wfvgn@igc.phys.chem.ethz.ch.

Notes

The authors declare no competing financial interest.

ACKNOWLEDGMENTS

This work was financially supported by the National Center of Competence in Research (NCCR) in Structural Biology and by grant number 200020-137827 of the Swiss National Science Foundation and by grant number 228076 of the European Research Council (ERC), which is gratefully acknowledged.

REFERENCES

(1) Tozzini, V. *Curr. Opin. Struct. Biol.* **2005**, *15*, 144−150.
(2) Takada, S. *Curr. Opin. Struct. Biol.* **2012**, *22*, 130−137.
(3) Riniker, S.; Allison, J. R.; van Gunsteren, W. F. *Phys. Chem. Chem. Phys.* **2012**, *14*, 12423−12430.
(4) Neri, M.; Anselmi, C.; Cascella, M.; Maritan, A.; Carloni, P. *Phys. Rev. Lett.* **2005**, 95.
(5) Shi, Q.; Izvekov, S.; Voth, G. A. *J. Phys. Chem. B* **2006**, *110*, 15045−15048.
(6) Ayton, G. S.; Noid, W. G.; Voth, G. A. *Curr. Opin. Struct. Biol.* **2007**, *17*, 192−198.
(7) Masella, M.; Borgis, D.; Cuniasse, P. *J. Comput. Chem.* **2008**, *29*, 1707−1724.
(8) Michel, J.; Orsi, M.; Essex, J. W. *J. Phys. Chem. B* **2008**, *112*, 657−660.
(9) Rzepiela, A. J.; Louhivuori, M.; Peter, C.; Marrink, S. J. *Phys. Chem. Chem. Phys.* **2011**, *13*, 10437.
(10) Riniker, S.; van Gunsteren, W. F. *J. Chem. Phys.* **2012**, *137*, 044120.
(11) Riniker, S.; van Gunsteren, W. F. *J. Chem. Phys.* **2011**, *134*, 084110.
(12) Riniker, S.; Eichenberger, A. P.; van Gunsteren, W. F. *Eur. Biophys. J.* **2012**, *41*, 647−661.
(13) Riniker, S.; Eichenberger, A. P.; van Gunsteren, W. F. *J. Phys. Chem. B* **2012**, *116*, 8873−8879.
(14) Christ, C. D.; van Gunsteren, W. F. *J. Chem. Phys.* **2007**, *126*, 184110.
(15) Christ, C. D.; van Gunsteren, W. F. *J. Chem. Phys.* **2008**, *128*, 174112.
(16) Christ, C. D.; van Gunsteren, W. F. *J. Comput. Chem.* **2009**, *30*, 1664−1679.
(17) Christ, C. D.; van Gunsteren, W. F. *J. Chem. Theory Comput.* **2009**, *5*, 276−286.
(18) Riniker, S.; Christ, C. D.; Hansen, N.; Mark, A. E.; Nair, P. C.; van Gunsteren, W. F. *J. Chem. Phys.* **2011**, *135*, 024105.
(19) Lin, Z. X.; Liu, H. Y.; Riniker, S.; van Gunsteren, W. F. *J. Chem. Theory Comput.* **2011**, *7*, 3884−3897.
(20) Lin, Z.; Timmerscheidt, T. A.; van Gunsteren, W. F. *J. Chem. Phys.* **2012**, *137*, 064108.
(21) Hansen, N.; Dolenc, J.; Knecht, M.; Riniker, S.; van Gunsteren, W. F. *J. Comput. Chem.* **2012**, *33*, 640−651.
(22) Oostenbrink, C.; Villa, A.; Mark, A. E.; van Gunsteren, W. F. *J. Comput. Chem.* **2004**, *25*, 1656−1676.
(23) Berendsen, H. J. C.; Postma, J. P. M.; van Gunsteren, W. F.; Hermans, J. In *Intermolecular Forces*; Pullman, B., Ed.; Reidel: Dordrecht, The Netherlands, 1981; pp 331−342.
(24) Allen, M. P.; Tildesley, D. J. *Computer Simulation of Liquids*; Oxford University Press: New York, 1987.
(25) The GROMOS software package can be downloaded from http://www.gromos.net.
(26) Eichenberger, A. P.; Allison, J. R.; Dolenc, J.; Geerke, D. P.; Horta, B. A. C.; Meier, K.; Oostenbrink, C.; Schmid, N.; Steiner, D.; Wang, D. Q.; van Gunsteren, W. F. *J. Chem. Theory Comput.* **2011**, *7*, 3379−3390.
(27) Riniker, S.; Christ, C. D.; Hansen, H. S.; Hünenberger, P. H.; Oostenbrink, C.; Steiner, D.; van Gunsteren, W. F. *J. Phys. Chem. B* **2011**, *115*, 13570−13577.
(28) Kunz, A. P. E.; Allison, J. R.; Geerke, D. P.; Horta, B. A. C.; Hünenberger, P. H.; Riniker, S.; Schmid, N.; van Gunsteren, W. F. *J. Comput. Chem.* **2012**, *33*, 340−353.
(29) Schmid, N.; Christ, C. D.; Christen, M.; Eichenberger, A. P.; van Gunsteren, W. F. *Comput. Phys. Commun.* **2012**, *183*, 890−903.
(30) Berendsen, H. J. C.; Postma, J. P. M.; van Gunsteren, W. F.; DiNola, A.; Haak, J. R. *J. Chem. Phys.* **1984**, *81*, 3684−3690.
(31) Ryckaert, J. P.; Ciccotti, G.; Berendsen, H. J. C. *J. Comput. Phys.* **1977**, *23*, 327−341.
(32) Tironi, I. G.; Sperb, R.; Smith, P. E.; van Gunsteren, W. F. *J. Chem. Phys.* **1995**, *102*, 5451−5459.
(33) Hansen, H. S.; Hünenberger, P. H. *J. Chem. Theory Comput.* **2010**, *6*, 2622−2646.